Model Reduction and System Identification for Master Equation Control Systems

Martha A. Gallivan and Richard M. Murray
Division of Engineering and Applied Science
California Institute of Technology
Pasadena, CA 91125

Abstract

A master equation describes the continuous-time evolution of a probability distribution, and is characterized by a simple bilinear-like structure and an often-high dimension. We develop a model reduction approach in which the number of possible configurations and corresponding dimension is reduced, by removing improbable configurations and grouping similar ones. Error bounds for the reduction are derived based on a minimum and maximum time scale of interest. An analogous linear identification procedure is then presented, which computes the state and output matrices for a predetermined configuration set. These ideas are demonstrated first in a finite-dimensional model inspired by problems in surface evolution, and then in an infinite-dimensional film growth master equation.

1 Introduction

A master equation is a probabilistic differential equation that describes a system defined by discrete configurations. Master equations are useful in describing systems at small length scales when continuum assumptions break down, particularly when fluctuations are important. The number of discrete configurations is often very large, so instead of numerically integrating the master equation, stochastic realizations are obtained through kinetic Monte Carlo (KMC) simulations [1].

The states of the master equation are the probabilities of each configuration, which evolve according to the linear equation

$$\frac{d}{dt}P_H(t) = \sum_{H'} k^{H'\to H} P_{H'}(t) - \sum_{H'} k^{H\to H'} P_H(t), \quad (1)$$

where H and H' denote two of the n configurations of the system, $P_H(t)$ is the probability of being in H at time t, and $k^{H'\to H}$ is rate of transition from H' to H. We focus on the evolution of expected properties of the system, defined as

$$\langle Y\rangle(t) = \sum_{H} P_H(t) Y(H), \quad (2)$$

where Y is the quantity of interest, $Y(H)$ is the value of Y associated with configuration H, and $\langle Y\rangle(t)$ denotes the time-dependent expected value of Y. One acts on the system by altering the transition rates using physical inputs $\mathbf{u} \in \mathbb{R}^q$, resulting in the state-affine control system of equations (1) and (2).

We now reformulate this system by assembling the states into a single vector and by grouping terms having the same values of the transition rates, obtaining

$$\frac{d}{dt}\mathbf{x} = \sum_{i=1}^{m} k_i(\mathbf{u}) N_i \mathbf{x} \quad (3)$$

$$\mathbf{y} = C\mathbf{x} \quad (4)$$

where $\mathbf{x} = \{P_{H_1}, \ldots, P_{H_n}\} \in \mathbb{R}^n$ is the probability vector and $\mathbf{y} \in \mathbb{R}^p$ is the vector of expected outputs. The coefficients of the state and output matrices, $N_i \in \mathbb{R}^{n\times n}$ and $C \in \mathbb{R}^{p\times n}$, respectively, are obtained directly from equations (1) and (2), while the m unique transition rates are dependent on $\mathbf{u}$, but not on $\mathbf{x}$. Equations (3) and (4) are identical to (1) and (2)—only the notation is different. Note that $\mathbf{x}$ is a probability vector, such that $0 \le x_j \le 1, j = 1, \ldots, n$ and $\sum_{j=1}^{n} x_j = 1$. Similarly, each N_i is a stochastic matrix, in which columns sum to zero, diagonal elements are nonpositive, and off-diagonal elements are nonnegative.

We are motivated in this work by our interest in materials processing. Transition rates for an associated master equation have been enumerated [9], and are the basis of KMC simulations of surface evolution during thin film deposition and etching. It would be useful to have a more compact version of this master equation. In recent work by Gillespie [4], conditions are derived for which the discrete variable distinguishing configurations may be made continuous, allowing the passage to a stochastic Langevin equation. In constrast to the chemically-reacting systems studied by Gillespie, the transition rates for surface evolution are not smooth and do not satisfy the criterion [4]. We consider here a different approach to dimension reduction, in which the dimension of the probability vector is reduced by exploiting the system's linearity, and then develop an analogous system identication method requiring only a constrained linear least squares computation.

2 Model Reduction

We constrain our reduced-order model to also be a probabilistic system. Although this is restrictive, it also has many benefits, including the preservation of the neutral stability of the system (under constant inputs), which is not guaranteed under most model reduction techniques. Each new state retains a physical interpretation, as a probability of some configuration, and the linearity of the system is preserved. We explore here two means of reduction, the first in which individual configurations, and corresponding states, are removed, and a second in which similar configurations are grouped into a single state. Any configuration may initially be occupied, so one can never reduce the dimension while incurring no error. However, if we restrict our attention to particular initial conditions, outputs, ranges of inputs, and time scales of interest, it may be possible to reduce the number of configurations with little output error.

It is often true that one wishes to model the evolution of a system over a finite period of time t_f, and that one is only interested in the evolution with a time resolution of Δt. For convenience we set $n_t = t_f/\Delta t$ to be an integer. Constraining the input to be constant over each Δt, we may thus formulate the discrete-time system

$$A_{\mathbf{u}_j} \equiv \exp\left(\Delta t \sum_{i=1}^{m} k_i(\mathbf{u}_j) N_i\right) \quad (5)$$

$$\mathbf{x}_d[j+1] = A_{\mathbf{u}_j}\mathbf{x}_d[j] \quad (6)$$

$$\mathbf{y}_d[j] = C\mathbf{x}_d[j], \quad (7)$$

where $j = 0, 1, \ldots, n_t$ increments the time, $A_{\mathbf{u}_j} \in \mathbb{R}^{n\times n}$ is the time-dependent state matrix, and $\mathbf{x}_d[j] \in \mathbb{R}^n$ and $\mathbf{y}_d[j] \in \mathbb{R}^p$ are the discrete-time state and output.

We now seek a state matrix $\tilde{A}_{\mathbf{u}} \in \mathbb{R}^{n\times n}$ that approximates $A_{\mathbf{u}}$, is also based on a master equation, and will admit the elimination or grouping of configurations (and consequent reduction in state dimension) with no error incurred. Both $A_{\mathbf{u}}$ and $\tilde{A}_{\mathbf{u}}$ are stochastic matrices, with nonnegative elements and column sums of one. Using this property, we may analyze the difference between the evolution of equations (6) and (7) and an analogous approximating system with $\tilde{A}_{\mathbf{u}}$, C, $\tilde{\mathbf{x}}_d \in \mathbb{R}^n$, and $\tilde{\mathbf{y}}_d \in \mathbb{R}^p$. Comparing the states using the one-norm, we obtain

$$\begin{aligned}
&\|\mathbf{x}_d[j+1] - \tilde{\mathbf{x}}_d[j+1]\|_1 = \|A_{\mathbf{u}_j}\mathbf{x}_d[j] - \tilde{A}_{\mathbf{u}_j}\tilde{\mathbf{x}}_d[j]\|_1 \\
&= \|A_{\mathbf{u}_j}\mathbf{x}_d[j] - \tilde{A}_{\mathbf{u}_j}\mathbf{x}_d[j] + \tilde{A}_{\mathbf{u}_j}\mathbf{x}_d[j] - \tilde{A}_{\mathbf{u}_j}\tilde{\mathbf{x}}_d[j]\|_1 \\
&\leq \|A_{\mathbf{u}_j}\mathbf{x}_d[j] - \tilde{A}_{\mathbf{u}_j}\mathbf{x}_d[j]\|_1 + \|\tilde{A}_{\mathbf{u}_j}\mathbf{x}_d[j] - \tilde{A}_{\mathbf{u}_j}\tilde{\mathbf{x}}_d[j]\|_1 \\
&\leq \|A_{\mathbf{u}_j} - \tilde{A}_{\mathbf{u}_j}\|_1\|\mathbf{x}_d[j]\|_1 + \|\tilde{A}_{\mathbf{u}_j}\|_1\|\mathbf{x}_d[j] - \tilde{\mathbf{x}}_d[j]\|_1 \ .
\end{aligned}$$

Using the fact that $\|\mathbf{x}_d[j]\|_1 = 1$ and $\|\tilde{A}_{\mathbf{u}_j}\|_1 = 1$, and defining $\epsilon_{\mathbf{u}_j} \equiv \|A_{\mathbf{u}_j} - \tilde{A}_{\mathbf{u}_j}\|_1$, we obtain a recursive equation for the bound

$$\|\mathbf{x}_d[j+1] - \tilde{\mathbf{x}}_d[j+1]\|_1 \leq \epsilon_{\mathbf{u}_j} + \|\mathbf{x}_d[j] - \tilde{\mathbf{x}}_d[j]\|_1. \quad (8)$$

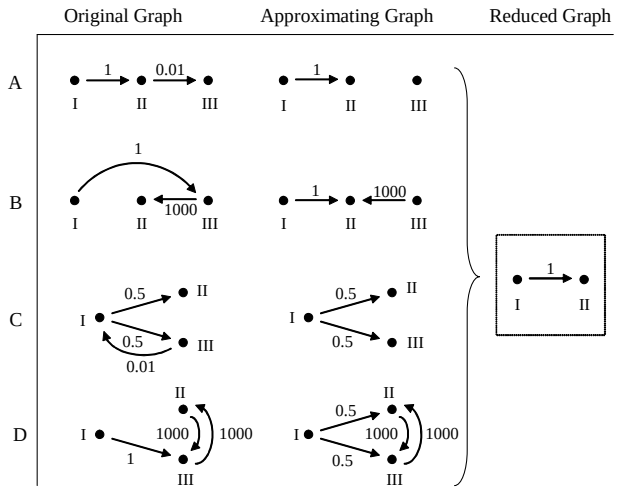

Figure 1: Four examples of physical mechanisms underlying configuration reduction. The dots denote configurations, with arrows denoting transitions with their rates.

Thus, with each additional time step j, the maximum additional error incurred is $\epsilon_{\mathbf{u}_j}$. Because we are only considering a maximum time of t_f, we may impose a maximum acceptable value on $\epsilon_{\mathbf{u}_j}$ to ensure that the error after $t_f/\Delta t$ time steps is sufficiently small.

It is clear that if $\tilde{A}_{\mathbf{u}}$ is close to $A_{\mathbf{u}}$, as measured by the one-norm, then little error is incurred by using the approximating map. Such ideas have been previously developed in the context of homogeneous Markov chains, particularly in the economics community [5, 8]. However, we are interested in controlled systems, and have developed the bound of equation (8) that enables straightforward consideration time-varying inputs.

Configurations may be truncated from a master equation if they are decoupled from the states in which the system is initially occupied. In other words, if $A_{\mathbf{u}}$ is a block-diagonal matrix, then there is no coupling between states belonging to different blocks, so if the system does not begin in a block, it will never enter it. When this is only approximately true for $A_{\mathbf{u}}$, we may then formulate an $\tilde{A}_{\mathbf{u}_j}$ in which it is exactly true. Two examples of approximate decoupling are shown in Figure 1, as A and B. For all the examples in this figure, we consider a maximum time $t_f = 10$, with $\Delta t = 0.1$, and also assume that the system begins in configuration I. The original graph of A shows a transition of rate 1 from I to II, and a much slower transition with rate 0.001 from II to III. Over the time interval of interest, we would not expect signficant transitions from II to III, and thus construct an approximating graph in which the transition from II to III has been removed. Configuration III is now decoupled from I and II, and since we begin in I, III will never be occupied, and may thus be eliminated from the master equation, resulting

in the reduced graph on the right of Figure 1. The error associated with the approximating map is $\epsilon = 2 \times 10^{-4}$ for these transition rates, so over $n_t = 100$ time steps, we would incur an error no greater than 2×10^{-2} in the probability distribution. Example B of Figure 1 also results in a near decoupling of $A_{\mathbf{u}}$, not because of a slow transition, but rather because of a transition much faster than Δt. After each interval of Δt the system will not occupy III with any significant probability, so an approximating map is constructed in which the transition from I to III is replaced by a transition from I to II. In this case, we get $\epsilon = 3 \times 10^{-3}$, and again obtain the reduced graph on the right of Figure 1.

Another method of configuration reduction is through the grouping of configurations. In example C, II and III are similarly coupled to the rest of the system, and therefore evolve similarly. In the approximating graph, the coupling is made identical, resulting in redundant configurations that may be grouped, yielding $\epsilon = 2 \times 10^{-3}$. One may search for potential groupings by observation of $A_{\mathbf{u}}$. If the columns corresponding to the two states are identical, and the rows are identical up to a constant factor, then the states evolve in a fixed ratio and may be grouped via a coordinate transformation [6], yielding the reduced graph in Figure 1. A second example of grouping is shown as D, in which two configurations are tightly coupled to each other, and achieve their equilibrium ratio at times less than Δt. In this limit, the corresponding columns of $A_{\mathbf{u}}$ are equal, with corresponding rows differing by their equilibrium ratio, so as in example C, they may be grouped, as shown in the approximating graph, with $\epsilon = 4 \times 10^{-4}$, and again, with the reduced graph in the box on the right side of Figure 1.

The reduction process has a straightforward physical interpretation, but also may be automated, by inspecting $A_{\mathbf{u}}$ for all $\mathbf{u}$'s in the set of allowable inputs. Configurations may be eliminated if the system can be decoupled, and may be grouped if they have similar columns and rows. We note that many of the physical arguments used in the examples rely on the separation of time scales, and therefore require that the transition rates are constrained via input constraints. This is entirely consistent with the establishment of t_f and Δt, since the transition rates scale the time in equations (1) and (3). We also note that other configuration reduction approaches, like singular perturbation [7], are possible, but may not preserve the structure of the master equations, which we exploit in the system identification.

3 System Identification

The state and output matrices of the reduced master equation may be determined by constructing an approximating graph, or by performing coordinate transformations on the master equation. This is straightforward when the system dimension is small, but for large systems, it might be desirable to determine the coefficents using a data-driven system identification approach. We develop here an approach that relies on the linearity of the system, and that requires only that the reduced configuration set be known.

The master equation does not contain a purely linear input, so frequency-response methods to linear system identification are not applicable. However, we may use an impulse-response approach, in which the impulsive inputs are replaced by appropriate initial conditions. We approximate equations (3) and (4) by a Taylor expansion, with small Δt, to obtain

$$\hat{A}_{\mathbf{u}_j} \equiv I(n) + \Delta t \sum_{i=1}^{m} k_i(\mathbf{u}_j) N_i \tag{9}$$

$$\mathbf{x}_d[j+1] = \hat{A}_{\mathbf{u}_j} \mathbf{x}_d[j] \tag{10}$$

$$\mathbf{y}_d[j] = C\mathbf{x_d}[\mathbf{j}], \tag{11}$$

where $I(n) \in \mathbb{R}^{n \times n}$ is the identity matrix, and $\mathbf{x}_d \in \mathbb{R}^n$, $\mathbf{y}_d \in \mathbb{R}^p$, $\hat{A}_{\mathbf{u}_j} \in \mathbb{R}^{n \times n}$, and C form a discrete-time version of the master equation.

The identification is based on the construction of an observability matrix for a particular fixed value of $\mathbf{u}$, where

$$\mathcal{O}_{\mathbf{u}} = \begin{bmatrix} C \\ C\hat{A}_{\mathbf{u}} \\ C\hat{A}_{\mathbf{u}}^2 \\ \vdots \\ C\hat{A}_{\mathbf{u}}^{n_t} \end{bmatrix}. \tag{12}$$

Simulations are performed for n_t time steps, beginning with the n initial conditions of $e_i, i = 1, ...n$, where element i of $e_i \in \mathbb{R}^n$ is one, and all others zero. This is equivalent to performing stochastic KMC simulations, in which the system begins in each of the n configurations. In either case, the simulation beginning in the i^{th} configuration generates the i^{th} column of $\mathcal{O}_{\mathbf{u}}$. The output matrix C can be extracted as the first block of $\mathcal{O}_{\mathbf{u}}$, while $\hat{A}_{\mathbf{u}}$ may be determined in a linear least squares computation, using the shift property of $\mathcal{O}$:

$$\mathcal{O}_{\mathbf{u}}(1, \ldots, n_t - 1)\hat{A}_{\mathbf{u}} = \mathcal{O}_{\mathbf{u}}(2, \ldots, n_t), \tag{13}$$

where the argument of $\mathcal{O}_{\mathbf{u}}$ is used to denote blocks of the original matrix.

The linear least squares computation is guaranteed to give the globally-optimal solution for $\hat{A}_{\mathbf{u}}$, in which the two-norm of the residual is minimized. However, this may not be the optimal solution for our application. The state matrices are discrete-time stochastic matrices, in which the columns sum to one, and all elements are nonnegative. These properties guarantee the conservation of probability, and may be enforced through linear equality and inequality constraints in a *constrained* linear least squares solution to equation (13). When Δt is small, this also enforces the stochastic properties of the N_i in continuous time. An element $\hat{A}_{\mathbf{u}}(p, q)$ may

also be set to zero using additional equality constraints, to eliminate the possibility of a transition from configuration p to configuration q. Such a constraint would typically be justified based on physical arguments.

This identification algorithm produces $\hat{A}_{\mathbf{u}}$, but does not independently yield the state matrices N_i. However, because $\hat{A}_{\mathbf{u}}$ is linear in N_i (see equation (9)), and because $k_i(\mathbf{u})$ is known, several observability matrices may be constructed for different (but constant) transition rates, which are then assembled into a single constrained linear least squares problem, yielding the coefficients in $N_i, i = 1, ...m$.

The linear least-squares computation yields a solution with the minimum two-norm of the residual, but if the problem is underconstrained, this solution may not be unique. The condition for unique determination of $\hat{A}_{\mathbf{u}}$ depends not only on the rank of $\mathcal{O}_{\mathbf{u}}$, but also on the equality constraints imposed. We suggest only that if the problem is underdetermined, one could either used more data in the identification, select additional outputs to provide more information about the state, or perhaps reduce the number of configurations, if some are redundant or are not contributing to the output. Alternatively, if the problem is underdetermined, then the connectivity implied by the least squares solution to $\hat{A}_{\mathbf{u}}$ may be sufficient to describe the output of interest.

4 Example 1: sixteen-state system

We now demonstrate the model reduction and system identification techniques developed in the previous sections on an example motivated by our interest in surface evolution. We consider a one-dimensional surface consisting of ten atomic sites, with five atoms located on the surface. The surface evolves as the atoms hop to adjacent empty sites. Figure 2 shows the sixteen unique configurations of the surface. Periodic boundary conditions are assumed, so configurations differing by only a translation or a reflection are not distinguished. Configurations are characterized by the number and relative location of monomers (single atoms with no neighbors) and clusters (groups of at least two adjacent atoms). Configurations with the same number of monomers and clusters are contained within a single box in Figure 2, and are considered to be potential candidates for configuration grouping.

We create a master equation by considering two expected outputs—the numbers of monomers and islands—and two distinct types of transitions. In the first transition, a monomer hops to an adjacent empty site. This transition may occur from IIa to IIb, from IIb to IIa, or from IIa to I. All transitions of this form have the same rate, which is dependent on the (input) temperature. The second type of transition occurs when an atom hops off the edge of a cluster to an empty site, and provides a transition, for example, from VIa to IVa or from I to IIa. This transition rate is less than for monomer hopping, since the extra atomic bond associated with the cluster makes the atom less mobile.

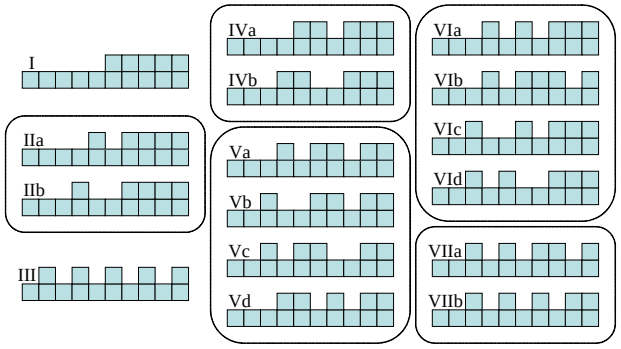

Figure 2: Sixteen unique configurations of a ten-site surface with five atoms. The configurations are grouped according to the number of monomers and clusters.

Table 1: Values of the error bound ϵ in equation (8) for two sets of transition rates and for three reductions.

	$\{k_1, k_2\} = \{10^4, 10\}\ s^{-1}$	$\{k_1, k_2\} = \{10^3, 0.5\}\ s^{-1}$
Group IIa & IIb, Va & Vb	9.3×10^{-4}	6.5×10^{-4}
Eliminate III, VI, VII	1.2×10^{-3}	9.3×10^{-4}
Both	2.1×10^{-3}	1.5×10^{-3}

We now consider a minimum time resolution of $\Delta t = 0.1\ s$, a maximum time $t_f = 10\ s$, and two sets of transition rates: $\{10^4, 10\}\ s^{-1}$ and $\{10^3, 0.5\}\ s^{-1}$. The first rate in each pair is the monomer hopping rate, while the second is for detachment from a cluster. For each set of transition rates, we compute ϵ associated with various configuration reductions. The results are given in Table 1. We first group the configuration pairs {IIa, IIb} and {Va, Vb}, since they are tightly coupled through monomer hopping transitions, resulting in dimension reduction from sixteen to fourteen. The effect of eliminating configurations in the groups III, VI, and VII is also reported, reducing the dimension from sixteen to nine. These configurations are unlikely to be occupied in the case when the monomer hopping rate is much greater than the cluster detachment rate. We finally present the error associated with both the grouping and the configuration elimination, and produce a seven-state system with the error given in Table 1.

We next apply the identification algorithm to the reduced-order master equation. We generate the simulation data by numerically integrating the master equation, and then adding to each element a random number of maximum magnitude 10^{-5}. The time step for the simulations is $0.1\ s$, with $n_t = 5$. Transition rates of $\{1, 1\}\ s^{-1}$ and $\{0, 1\}\ s^{-1}$ are used in the simulations, so that the time scale of the transients is consis-

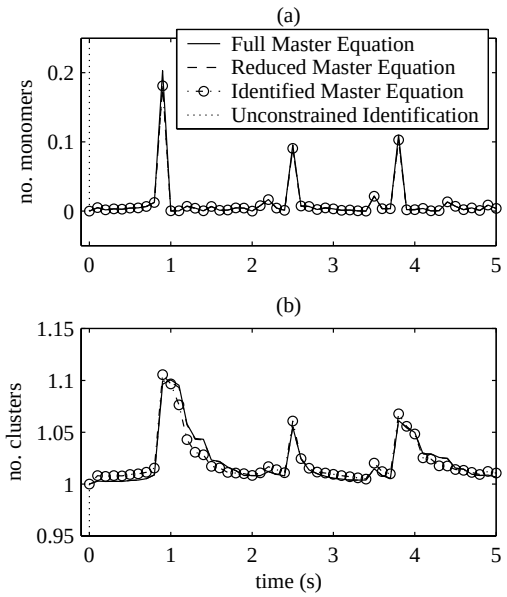

Figure 3: Comparison of the original equation of example 1 to its reduced-order version, and to two identified models.

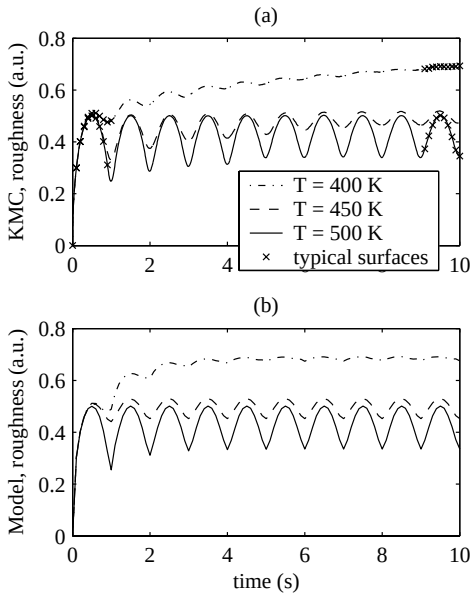

Figure 4: (a) Individual KMC simulations at three constant temperatures. (b) Reduced-order model under the same temperatures.

tent with the time step. We thus construct two observability matrices and perform a single constrained linear least squares computation to generate the output matrix, and a state matrix for each of the two transition mechanisms. Two different identified models are computed, one in which the state matrices are constrained to be stochastic, and another with no constraints at all.

The identified systems are compared to both the original system and to the reduced master equation, under the same set of random inputs and beginning in configuration I. The transition rates take new values at each time step of 0.1 s, with a monomer hopping rate between 0 and 10^4 s^{-1}, and a cluster detachment rate between 0 and 10 s^{-1}. The results are shown in Figure 3. The identified model generated by constrained linear least squares compares well with the reduced and full master equations. The difference in performance between the identified master equation and the (unstable) unconstrained system is striking, but should not be surprising. Since the state matrices of a master equation are stochastic, they contain at least one eigenvalue at the origin. If the eigenvalues of the identified matrices are not constrained in some way, any noise added to the simulation data may lead to one or more unstable eigenvalues in the identified system. While, in general, constraining the eigenvalues of a matrix in a linear computation is nonlinear, the eigenvalues of a stochastic matrix are never unstable. This point turns out to be critically important in our identification method.

5 Example 2: infinite-dimensional system

We are ultimately interested in reducing the dimension associated with large two-dimensional surfaces during film growth. In this case each surface site may take any integer height, yielding an infinite number of configurations. Our simulations are described in further detail in [2, 3]. We consider transitions for the adsorption of a new atom onto the surface, with rate $k_{\text{ads}} = 1\ s^{-1}$, and atom hopping, or diffusion, with rate $k_{\text{dif},i} = 10^{13} \exp\left((E_{\text{dif},0} + i\Delta E)/k_b/T\right)\ s^{-1}$, where $E_{\text{dif},0}/k_b = 9000\ K$, $\Delta E/k_b = 2500\ K$, and i is the number of side bonds for each atom. The temperature is restricted to the range $400 \leq T \leq 500\ K$, and a surface with 300×300 sites is used.

To generate a reduced model, the finite configuration set must first be established. Due to the infinite number of original configurations, individual configurations are not grouped or eliminated, but instead we select a finite number of typical, representative configurations, based on our understanding of the physics. Each configuration in this finite set is intended to represent a group of configurations with similar statistics that evolve together. Unimportant configurations are impliciting eliminated if they are not associated with one of these groups.

Kinetic Monte Carlo simulations at 400, 450, and 500 K are shown in Figure 4(a). The 'x's mark the configurations selected for the configuration set. Observability matrices are then constructed for each of these three temperatures from individual simulations to generate three discrete-time state matrices $A_{\mathbf{u}}$, associated with each temperature. We do not generate the individual

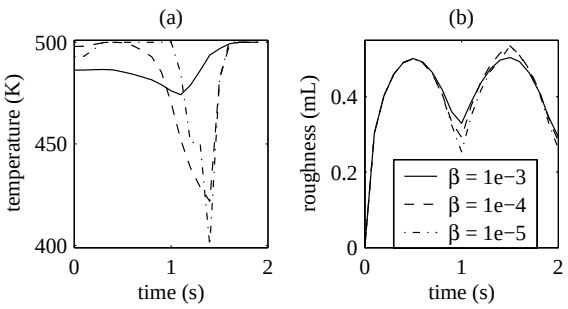

Figure 5: Results of optimization: (a) Optimized temperature profile. (b) Simulation of reduced-order model under optimized temperature.

N_i, but instead interpolate between the $A_{\mathbf{u}}$ for intermediate temperatures. Simulations of this 80-state model are shown in Figure 4(b), demonstrating good qualitative and quantitative agreement.

We now use the reduced-order model to compute the optimal temperature profiles to minimize the cost function $Cost = W(N) + \beta \sum_{j=1}^{N-1} (T_j - T_{j+1})^2$, where N is the number of time steps, $W(N)$ is the final roughness, and β is the cost for fast temperature change. We consider three values of β, and compute the optimal temperature over two layers of growth, with results shown in Figure 5. When the penalty on temperature change is large, the optimal strategy is to keep the temperature high, but for small penalties, the best approach is to lower the temperature at the beginning of the final layer to create many small clusters, and then raise the temperature to fill in the gaps between clusters. It would be impractical to perform this type of analysis directly on the KMC simulations. Further discussion of the relative computational costs is available in [2], in which the simulation cost of the reduced-order model is 3-4 orders of magnitude less than the KMC simulations.

6 Discussion and Conclusions

Master equations describe many systems of interest, including chemical reactions and surface evolution. The number of discrete configurations is often large or infinite. However, the behavior observed in the evolution of expected properties may not require this high dimension, either because some configurations are improbable or because redundant configurations or paths exist. We have developed here an error bound between an original and a reduced-order master equation. The bound depends only on the differences in the exponential operators over one time step, and the number of time steps executed. A system identification procedure is then presented. Only the configuration set must be known *a priori*, which may either be the original data set, or a reduced configuration set. Simulation data is then used to generate the state and output matrices. The reduction and identification methods are demonstrated in a sixteen-state master equation based on surface evolution. We have also considered much larger surfaces (300×300 sites) evolving during thin film deposition. In this example the number of configurations is infinite, as atoms are continually deposited on the surface. Instead of formally reducing the system dimension via coordinate transformations and computing error bounds for the reduction, we simply postulate a representative configuration set. Kinetic Monte Carlo simulations are then performed to generate the corresponding state and output matrices. The identified models compare well with the original KMC simulations, and can be used to compute optimal input trajectories.

We conclude that master equations are an important class of control systems, particularly for physical systems at small length scales, and that their often high dimension may be reduced. We have presented in this work complementary model reduction and system identification methods for finite-dimensional master equations that capture the dominant dynamics with a reduced dimension. These approaches also suggest a path for reducing infinite-dimensional master equations to low-order models.

Acknowledgments

This work was supported by DARPA and NSF under grant DMS-9615858, by AFOSR under grant AFOSR-F49620-95-1-0419, by ARO under grant DAAD19-01-1-0517, and by an NSF graduate fellowship.

References

[1] K. A. Fichthorn and W. H. Weinberg. Theoretical foundations of dynamical Monte Carlo simulations. *Journal of Chemical Physics*, 95:1090–1096, 1991.

[2] M. A. Gallivan. *Modeling and Control of Epitaxial Thin Film Growth*. PhD thesis, California Institute of Technology, Pasadena, CA 91125, September 2002.

[3] M. A. Gallivan, D. G. Goodwin, and R. M. Murray. Modeling and control of thin film morphology using unsteady processing parameters: problem formulation and initial results. In *Proceedings of the 40th IEEE Conference on Decision and Control*, pages 1570–1576, 2001.

[4] D. T. Gillespie. The chemical Langevin equation. *Journal of Chemical Physics*, 113(1):297–306, 2000.

[5] J. G. Kemeny and J. L. Snell. *Finite Markov Chains*, page 123. D. Van Nostrand Company, Inc., Princeton, New Jersey, 1960.

[6] O. Lange. *Price Flexibility and Employment*, pages 103–109. The Principia Press, Bloomington, Indiana, 1952.

[7] R. G. Phillips and P. V. Kokotovic. A singular perturbation approach to modeling and control of Markov chains. *IEEE Transactions on Automatic Control*, 26(5):1087–1094, 1981.

[8] H. A. Simon and A. Ando. Aggregation of variables in dynamic systems. *Econometrica*, 29(2):111–138, 1961.

[9] D. D. Vvedensky, A. Zangwill, C. N. Luse, and M. R. Wilby. Stochastic-equations of motion for epitaxial-growth. *Physical Review E*, 48:852–862, 1993.